N72-~~10045~~ 19758

SPACE RESEARCH COORDINATION CENTER



DISSOCIATIVE EXCITATION OF VACUUM ULTRAVIOLET EMISSION FEATURES BY ELECTRON IMPACT ON MOLECULAR GASES III. CO_2

CASE FILE COPY

BY

M. J. MUMMA, W. L. BORST, AND E. C. ZIPF

SRCC REPORT NO. 162

UNIVERSITY OF PITTSBURGH
PITTSBURGH, PENNSYLVANIA

JANUARY 1972

The Space Research Coordination Center, established in May, 1963, has the following functions: (1) it administers predoctoral and postdoctoral fellowships in space-related science and engineering programs; (2) it makes available, on application and after review, allocations to assist new faculty members in the Division of the Natural Sciences and the School of Engineering to initiate research programs or to permit established faculty members to do preliminary; work on research ideas of a novel character; (3) in the Division of the Natural Sciences it makes an annual allocation of funds to the interdisciplinary Laboratory for Atmospheric and Space Sciences; (4) in the School of Engineering it makes a similar allocation of funds to the Department of Metallurgical and Materials Engineering and to the program in Engineering Systems Management of the Department of Industrial Engineering; and (5) in concert with the University's Knowledge Availability Systems Center, it seeks to assist in the orderly transfer of new space-generated knowledge in industrial application. The Center also issues periodic reports of space-oriented research and a comprehensive annual report.

The Center is supported by an Institutional Grant (NsG-416) from the National Aeronautics and Space Administration, strongly supplemented by grants from the A. W. Mellon Educational and Charitable Trust, the Maurice Falk Medical Fund, the Richard King Mellon Foundation and the Sarah Mellon Scaife Foundation. Much of the work described in SRCC reports is financed by other grants, made to individual faculty members.

DISSOCIATIVE EXCITATION OF VACUUM ULTRAVIOLET EMISSION FEATURES BY ELECTRON IMPACT ON MOLECULAR GASES*+

III. CO_2

(Submitted to Journal of Chemical Physics)

M. J. Mumma+, W. L. Borst**, and E. C. Zipf

Physics Department, University of Pittsburgh

Pittsburgh, Pennsylvania 15213

January 1972

"Approved for public release; distribution unlimited."

DISSOCIATIVE EXCITATION OF VACUUM ULTRAVIOLET EMISSION FEATURES BY ELECTRON IMPACT ON MOLECULAR GASES*+

III. CO_2

M. J. Mumma‡, W. L. Borst**, and E. C. Zipf
Physics Department, University of Pittsburgh
Pittsburgh, Pennsylvania 15213

ABSTRACT

Vacuum ultraviolet multiplets of CI, CII, and OI have been produced by electron impact on CO_2. Absolute emission cross sections for these multiplets have been measured from threshold to 350 eV. The electrostatically focussed electron gun used in this series of experiments is described in detail. The atomic multiplets which were produced by dissociative excitation of CO_2 and the cross sections at 100 eV are: OI($2p^4\ ^3P$ - $2p^3 3s\ ^3S$) 1304Å - 1.04×10^{-18} cm^2 ±18%; CI($2s^2 2p^2\ ^3P$ - $2s2p^3\ ^3P^o$) 1329Å - $2.67 \times 10^{-19} cm^2$ ± 21%; CI($2s^2 2p^2\ ^3P$ - $2s2p^3\ ^3D^o$) 1561Å - 7.50×10^{-19} cm^2 ± 30%; CI($2p^2\ ^3P$ - $2p3s\ ^3P^o$) 1657Å - $1.45 \times 10^{-18} cm^2$ ± 23%; CII($2s^2 2p\ ^2P^o$ - $2s2p^2\ ^2D$) 1335Å - $7.60 \times 10^{-19} cm^2$ ± 22%; and CII($2s2p^2\ ^2D$ - $2p^3\ ^2D^o$) 1324Å - 1.33×10^{-20} cm^2 ± 23%. The dependence of the excitation functions on electron energy shows that these multiplets are produced by electric-dipole-allowed transitions in CO_2.

INTRODUCTION

In parts I and II of this series, we described dissociative excitation of atomic multiplets of HI, OI, and NI by electron impact on H_2, O_2, and N_2, respectively.[1,2] Excitation of the CO fourth positive group by electron impact on CO and on CO_2 was also studied.[3,4] In this paper we present absolute cross sections for dissociative excitation of CO_2 to yield multiplets of CI, CII, and OI in the vacuum ultraviolet.

The measurements on CO_2 were inspired by the then-imminent ultraviolet spectroscopic observations of the Mars upper atmosphere by the Mariner 6 and 7 spacecraft. The multiplets discussed in this paper were found to be prominent features of the Mars dayglow. Barth et al[5] have shown that they are produced in the Mars upper atmosphere by the action of solar photons and photoelectrons on CO_2. The cross sections presented here have been utilized by McConnell and McElroy[6] to perform detailed calculations of the CI 1657 Å and CI 1561 Å emissions in the dayglows of Venus and Mars.

The dissociative excitation of CO_2 has been studied concurrently with this work by Ajello[7] and Sroka.[8]

EXPERIMENT

The experiment featured an electrostatically focussed electron beam which was varied in energy from ~ 5 eV to 350 eV. Photons were collected at right angles to the electron beam by a McPherson Model 225 monochromator and an EMR 541G-08-18 solar-blind photomultiplier tube. Coherent summing techniques were used to improve the statistics of the data. The experimental techniques and apparatus have been described in detail elsewhere,[1,9,10] with the exception of the electron gun, which we describe here.

The electron gun was electrostatically focussed[11] and made use of the multistage principle.[12] The gun configuration is shown schematically in Fig. 1. Electrons from a thoria coated iridium filament F were accelerated through an aperture in the grid G towards anode A and electrode L. The electrons were then decelerated to their final energy by the potential on electrode P and the gun housing. The collision chamber was at the same potential as the gun housing. High potentials on electrodes A and L served to reduce the space charge in front of the cathode. This yielded relatively high beam currents at low energy.

The electron gun used was a modified oscilloscope gun (Superior Electronics Corp., Model SE-2B). The modifications performed consisted in a change of the aperture sizes and a different electrical mode of operation. The modified aperture sizes and potentials applied to the electrodes are listed in Table I. These potentials for the optimum focussing conditions were obtained by trial and error and are approximate. The final energy of the electrons in the collision chamber was eV_o.

For convenience, the potential on electrode L was chosen to be the same as that on A. A slightly different potential on L may result in even better focussing. All potentials were obtained from a single voltage supply by potentiometric division. This assured optimum focussing without readjustment at all electron energies in question.

The electron gun was operated in the energy range 5 to 400 eV and delivered a beam current of several microamperes. The current usually increased with energy. However the current-voltage characteristic could be made rather flat by optimizing the electrode potentials. The electron beam through the collision chamber was well collimated. The current to the collision chamber walls was generally less than 1% of the focussed current monitored at the electron collector (Faraday cup). The energy spread in the beam was about 0.5 eV (FWHM) as determined from the threshold behavior of excitation functions. The beam diameter was about 1 mm and was estimated from the spatial extent of luminosity resulting from electron impact excitation of gases in the collision chamber.

RESULTS

OI 1304Å Multiplet

The OI($2p^4\ ^3P$-$2p^3 3s\ ^3S$) transition is the first resonance transition of atomic oxygen and consists of lines at 1302.17, 1304.87, and 1306.04A°.[13] This multiplet was excited by the impact of 100 eV electrons on CO_2 and the spectral region 1280 - 1320Å was scanned at 0.8Å resolution. The detectable emission feature which was closest to the 1304Å multiplet was the CI 1311Å line. The monochromator was then centered on the OI 1304Å multiplet and the slits were set to yield 6Å resolution. The image of the 1304Å multiplet was included in the unity bandpass region of the monochromator transfer function. The CO_2 pressure in the collision chamber was $< 2\times10^{-4}$ torr and the electron beam current was $< 2\times10^{-5}$ amperes. The emission intensity was earlier found to be linear with pressure and current at these settings. The excitation function was measured and the cross section was later compared to the cross section for dissociative excitation of Lyman alpha (HI 1216Å) radiation by electron impact on H_2. The absolute cross section for the OI 1304Å multiplet is shown in Fig. 2.

The cross section exhibits an appearance potential at 21 eV ± 2 eV and a second feature at ~ 45 eV, then rises steeply to a broad maximum centered at 110 eV and then decreases monotonically as the energy increases to 350 eV. The shape of the cross section shows the excitation process is electric dipole allowed at higher energies. The absolute cross section at 100 eV is 1.0×10^{-18} cm^2 ± 18% (Table II).

The excitation cross sections of Ajello[7] and Sroka[8] are compared

with the results of this work in Figure 3 and Table III. All three curves are in good agreement regarding the appearance potential. There is agreement between Sroka and this work for the position of the second threshold (~45 eV) and between Ajello and this work regarding the position of the peak (~110 eV) and the shape at high energies. The disagreement in shape displayed by Sroka's results at high energies (> 100 eV) may stem from the effects of electrons backscattered along the collimating magnetic field in Sroka's experiment. The excitation functions presented in Parts I and II of this work exhibit shapes which are in good agreement with the results of other experimenters.[1,2] We have no reason to suspect that the shapes of the excitation functions for CO_2 are anomalous.

One might at first think that the dissociative process requiring the least energy to make $O(3s^3S)$ would be

$$e^- + CO_2(\tilde{X}\ ^1\Sigma_g^+) \rightarrow CO(X^1\Sigma^+) + O(3s^3S) + e^-, \qquad (1)$$

which requires at least 14.97 eV, i.e.

$$T_{min} = D_o^o(CO\text{-}O) + T_e(O^*) \qquad (2)$$

$$= 5.45 + 9.52 = 14.97 \text{ eV}.$$

However, correlation rules show that the intermediate CO_2^* state must be $^3\Sigma^-$ to yield the fragments shown in eqn. 1.[14] Since $\Sigma^+ \rightarrow \Sigma^-$ transitions are strictly forbidden, eq. 1 does not represent a physically important mechanism. The observed appearance potential is in good agreement with the mechanism (Table IV),

$$e^- + CO_2(X^1\Sigma_g^+) \rightarrow CO(a^3\Pi) + O(3s^3S) + e^-, \quad (3)$$

$$T_{min} = D_o^o(CO\text{-}O) + T_e(CO^*) + T_e(O^*)$$

$$= 5.45 + 6.01 + 9.52 = 20.98 \text{ eV}. \quad (4)$$

The $CO(a^3\Pi)$ state is the lowest triplet state and radiates the Cameron bands in the vacuum ultraviolet.

The second threshold (at 45 eV) probably corresponds to dissociative ionization and excitation following removal of a strongly bonding inner shell electron in CO_2 (see Discussion).

CI 1329Å Multiplet

The $CI(2s2p^3\ ^3P^o - 2s^22p^2\ ^3P)$ multiplet radiates lines at 1328.82Å, 1329.10Å, and 1329.58Å (Fig. 4).[13] The excitation function for the CI 1329 multiplet was measured at a monochromator bandpass of 4.15 Å after first determining that there were no other detectable emission features within this bandpass. The CO_2 pressure was $< 5\times10^{-4}$ torr and the electron beam current was $< 2\times10^{-5}$ amperes. The excitation function was put on an absolute scale at 100 eV by comparing it to the OI 1304 Å cross section which was described in the previous section (Table II). The absolute excitation cross section for the CI 1329 multiplet is shown in Fig. 5. The appearance potential (~24 eV) is only approximate since the counting statistics were poor (~10% at the peak). The observed appearance potential is compared to possible sets of states for the fragment species in Table IV.

The cross section rises steeply from threshold to a broad maximum centered at 100 eV and then decreases monotonically at higher energies. The shape is characteristic of an electric - dipole-allowed process. The scatter in the data is too great to determine whether these is a second threshold at ~45 eV.

CI 1561 Å Multiplet

The CI($2s2p^3\ ^3D^o \rightarrow 2s^2 2p^2\ ^3P$) multiplet radiates lines at 1560.31, 1560.70, 1561.29, and 1561.40Å (Fig. 4).[13] The CI 1561 multiplet was overlapped by the (1,1) and (4,3) bands of the CO fourth positive system which were excited by dissociative excitation of CO_2. The bandheads lie at 1560Å and the bands are degraded to longer wavelengths so that they overlap the entire multiplet. An excitation function was measured at 12Å resolution for the sum of the (1,1) band, the (4,3) band, and the CI 1561Å multiplet (Fig. 6). The appearance potential corresponds to the threshold for dissociative excitation of the v'=1 vibrational level of the $CO(A^1\pi)$ state, i.e.

$$e^- + CO_2(\tilde{X}^1\Sigma_g^+) \rightarrow CO(A^1\pi,\ v'=1) + O(^3P) + e\ , \qquad (5)$$

$$CO(A^1\pi) \rightarrow CO(X^1\Sigma^+) + h\nu_{1,1}\ ,$$

$$T_{min} = D_o^o(CO\text{-}O) + E_{v'=1} = 5.45 + 8.21 = 13.7\ eV.$$

The shape of the excitation function of the (1,1) band has been

reported elsewhere[3] and is shown by the dashed line in Fig. 6. The (4,3) band is only 1/10 as intense as the (1,1).

A second threshold occurs at ~26 eV and can tentatively be identified with the total dissociation process (Table IV)

$$e + CO_2(\tilde{X}^1\Sigma_g^+) \rightarrow C(2s2p^3\ {}^3D^o) + O(^3P) + O(^3P), \qquad (6)$$

$$C(^3D^o) \rightarrow C(^3P) + h\nu_{1561},$$

$$T_{min} = D_o^o(CO\text{-}O) + D_o{}^o(C\text{-}O) + E_{1561},$$

$$\approx 24.51 \text{ eV}.$$

The cross section rises steeply through a subsidiary maximum at ~38 eV to a third threshold at ~46 eV after which it rises to a broad maximum centered at 105 eV. The structure at 46 eV probably represents dissociative ionization by removal of an inner shell electron from the $3\sigma_g$ orbital of CO_2, as discussed in the section on OI. The absolute total cross section (bands + multiplet) was determined at 100 eV by comparing with the OI 1304 cross section and was found to be 9.7×10^{-19} cm^2 ±22% of which 7.5×10^{-19} cm^2 was due to the CI 1561 multiplet. The shape of the cross section at high energies is characteristic of an electric dipole allowed transition.

CI 1657Å Multiplet

The CI ($2p3s\ ^3P^o$ - $2p^2\ ^3P$) multiplet consists of lines at 1656.26, 1656.92, 1657.00, 1657.37, 1657.89, and 1658.11Å (Fig. 4).[13] The CI 1657 multiplet was overlapped by the (0,2) band of the CO fourth positive system which was excited by dissociative excitation of CO_2.

The excitation function for the sum of the (0,2) band and the CI 1657 multiplet was measured at 16.6Å resolution (Fig. 7). The appearance potential was 14 eV ± 2 eV in good agreement with the expected threshold (13.53 eV) for excitation of $CO(A^1\pi, v'=0)$ by the mechanism of eqn. 5. The shape of the excitation cross section for the CO 4^+ (1,1) band has been reported elsewhere[3] and is shown by the dashed line in Fig. 7. A second threshold occurs at ~25 eV and this is consistent with production of the CI 1657 multiplet by the total dissociation mechanism (Table IV) which requires at least 24.06 eV of energy (neglecting kinetic energy of the dissociation fragments). A third threshold occurs at ~50 eV and probably corresponds to dissociative ionization and excitation. The cross section rises to a broad maximum centered at ~110 eV and thereafter decreases with increasing energy. The shape is characteristic of an electric-dipole-allowed transition. The value of the total cross section at 100 eV is 1.5×10^{-18} cm^2 ± 22% of which 1.4×10^{-18} cm^2 is due to the CI 1657 multiplet.

CII 1335 Å Multiplet

The CII ($2s2p^2\ ^2D \rightarrow 2s^2 2p\ ^2P^0$) multiplet consists of lines at 1334.53, 1335.66, and 1335.71 Å(Fig. 4).[13] The excitation function (Fig. 8) was measured at 4.15 Å resolution and no other emission features were detected in this bandpass. The appearance potential is 44 ± 2 eV and is compared to possible states of the dissociation fragments in

Table IV. There are many possible sets of states which have $T_{min} < 44$ eV. The excess energy may be stored in the electronic structure of the oxygen atoms or may appear as kinetic energy. It cannot represent a cascade mechanism in the CII ion since the emission cross section of the CII 1324 multiplet was found to be less than 2% of the CII 1335 cross section at 100 eV (Table II). The CII 1335 cross section rises smoothly from threshold to a broad maximum which is centered at ~170 eV and then decreases monotonically at higher energies. The absolute value at 100 eV is 7.6×10^{-19} cm^2 ± 23% and the shape is characteristic of an electric-dipole-allowed transition.

The present data are compared with the data of Ajello[7] and Sroka[8] in Fig. 9 and Table V. The shapes are in good agreement but Sroka's absolute values differ by about a factor of two from Ajello's. Ajello's work and the present results are the preferred values since these experimenters utilized recently developed calibration techniques which enable accurate calibration of monochromators over the wavelength range 1100 - 2600 Å.

DISCUSSION

In this paper we have presented excitation cross sections (0 - 350eV) for multiplets of OI, CI, and CII by electron impact on CO_2. All of the observed excitation processes were electric-dipole-allowed at high energies. The OI 1304Å multiplet exhibits an appearance potential corresponding to the fragments CO and O. The CI and CII multiplets exhibit appearance potentials which are larger by several volts (~5) than the lowest

possible energy for producing $C + O_2$ or $C^+ + O_2$, respectively. Thus, if O_2 is a direct dissociation fragment, there is ~5 eV available for distribution among the fragments. The close agreement between the excess energy and the bond energy of O_2 suggests that the CO_2 fragments completely. The excitation function for the OI and CI multiplets exhibit secondary thresholds at ~45 eV while the CII 1335 multiplet exhibits an appearance potential at ~44 eV. This strongly suggests that these secondary thresholds and the CII appearance potential are consequences of dissociative ionization by the removal of a strongly bonding electron from an inner shell orbital of CO_2. This hypothesis is supported by the known characteristics of the molecular orbitals of CO_2.

The ground configuration of CO_2 may be written,

$$CO_2(\tilde{X}^1\Sigma_g^+)\ (1\sigma_g)^2(1\sigma_u)^2(2\sigma_g)^2(3\sigma_g)^2(2\sigma_u)(4\sigma_g)^2(3\sigma_u)^2(1\pi_u)^4(1\pi_g)^4. \quad (7)$$

The inner shell electrons have vertical ionization potentials of 13.8, 17.6, 18.1, and 19.4 eV, corresponding to removal of an electron from the $1\pi_g$, $1\pi_u$, $3\sigma_u$, and $4\sigma_g$ orbitals, respectively.[15] The next ionization limits of CO_2 have been calculated to be at 42 eV and 45 eV, corresponding to removal of an electron from the inner shell $2\sigma_u$ and $3\sigma_g$ orbitals, respectively. Measurements of the photoelectron spectrum of CO_2 have shown that the $1\pi_g$, $3\sigma_u$, and $4\sigma_g$ orbitals are non-bonding while the $1\pi_u$ orbital is strongly bonding in character.[15] These results confirmed the calculations of Peyerimhoff et al.[17] and showed that Mulliken's[18] original

classification of the bonding character of the σ - type orbitals was incorrect. Peyerimhoff's results also predicted that the orbitals $3\sigma_g$ and $2\sigma_u$ should be strongly bonding. The remaining orbitals ($2\sigma_g$, $1\sigma_u$, $1\sigma_g$) may be regarded as atomic orbitals ($1s_c$, $1s_o$, $1s_o$) and are very tightly bound, playing no further role in this discussion.

The $2\sigma_u$ orbital is composed primarily of ($2s_o$ - $2s_o$) character and removal of an electron from this orbital will result in an excited oxygen ion if the core CO_2^+ dissociates. The $3\sigma_g$ orbital can be written ($2s_o$ + $2s_c$ + $2s_o$) and dissociation following removal of an electron from the $3\sigma_g$ orbital will have a certain probability of producing a carbon ion with the configuration CII($1s^2 2s 2p^2$). We have observed production of this state (i.e. we observed the CII 1335Å multiplet) and found the appearance potential to be ~44 eV. The three independent measurements of the appearance potential are in agreement with a value of 45 eV (Table V). We conclude that the CII 1335Å multiplet is produced by removal of an electron from the $3\sigma_g$ orbital accompanied by dissociation of the core ion. Since the $3\sigma_g$ orbital is composed of a linear combination of atomic orbitals ($2s_o$, $2s_c$, and $2s_o$) we expect that removal of an electron from that orbital will have a certain probability to produce OII($1s^2 2s^2 p^4$) + OI + CI. Thus one expects to find radiation at 833.8Å [OII($2s2p^4$ - $2s^2 2p^3$)] with an appearance potential at 42 or 45 eV depending on whether dissociative ionization from the $2\sigma_u$ orbital also occurs. Sroka[8] observed an appearance potential of

~48 eV for this multiplet which suggests that only the $3\sigma_g$ orbital is involved near threshold.

The observed appearance potentials for the CI multiplets fall in the range 24-26 eV (Table IV). These processes must represent dissociative excitation through doubly excited valence states of CO_2 rather than through Rydberg states belonging to the known ionization limits since the Rydbergs of a given series lie within ~4 eV of the ionization limit. There are no Rydberg states between ~19.4 eV and ~38 eV. However, when the statistics of the data allowed a determination of the structure in the cross section, we found secondary thresholds at ~46 eV(CI 1561Å) and ~50 eV (CI 1657Å). These values may be high by several volts. The structure in the CI 1561Å cross section can be understood as excitation of a Rydberg state of the $3\sigma_g$ orbital which leaves the 2s electron of the carbon atom in the 2p level after dissociation.

CONCLUSION

In this series of papers we have described absolute cross sections for dissociative excitation of H_2, O_2, N_2, CO_2, and CO by electron impact to yield vacuum ultraviolet features in the wavelength range 1165 - 1900Å. These data were needed for calculations of the primary production rates of these features by secondary electrons in disturbed planetary atmospheres[19] (aurora) and by photoelectrons in the dayglows of Mars and Venus.[6] In addition to the practical applications of these results, they provide insight for better

understanding the phenomena of molecular dissociation and demonstrate the need for careful experimental probing of molecular states (stable and unstable) above the first ionization limit.

FOOTNOTES AND REFERENCES

*This research was supported by the Advanced Research Project Agency, The Department of Defense, and was monitored under Contract No. DA-31-124-ARO-D-440 and by the National Aeronautics and Space Administration (NGL 39-011-030).

+Preliminary results of this work were presented at the 22nd Gaseous Electronic Conference (27-31 October 1969), Gatlinburg, Tennessee [Bull. Am. Phys. Soc. 15, 422 (1970)].

‡ Present Address: Astrochemistry Branch, Code 691, Laboratory for Extraterrestrial Physics, NASA/Goddard Space Flight Center, Greenbelt, Maryland 20771.

**Present Address: Department of Physics, Southern Illinois University, Carbondale, Illinois 62901.

1. M. J. Mumma and E. C. Zipf, J. Chem. Phys. 55, 1661 (1971).

2. M. J. Mumma and E. C. Zipf, J. Chem. Phys. 55, 0000 (1971).

3. M. J. Mumma, E. J. Stone, and E. C. Zipf, J. Chem. Phys. 54, 2627 (1971).

4. M. J. Mumma, E. J. Stone, and E. C. Zipf, Abstracts VIIth Intl. Conf. Physics of Electronic and Atomic Collisions, (North-Holland), 858 (1971).

5. C. A. Barth, C. W. Hord, J. B. Pearce, K. K. Kelly, G. P. Anderson, and A. I. Stewart, J. Geophys. Res. 76, 2213 (1971).

6. M. B. McElroy and J. C. McConnell, J. Geophys. Res. 76, 6674 (1971).

7. J. Ajello, J. Chem. Phys. 55, 3169 (1971).

8. W. Sroka, Z. Naturforsch. 25a, 1434 (1970).

9. M. J. Mumma, Dissociative Excitation of Atmospheric Gases, Ph.D. Thesis, University of Pittsburgh (1970).

10. M. J. Mumma and E. C. Zipf, J. Opt. Soc. Am. 61, 83 (1971).

11. A similar electron gun was briefly described by W. L. Borst and E. C. Zipf, Phys. Rev. 1, 834 (1970). A more detailed description is presented in this paper.

12. J. A. Simpson and C. E. Kuyatt, Rev. Sci. Instr. 34, 265 (1963).

13. W. L. Wiese, M. W. Smith, and B. M. Glennon, Natl. Std. Ref. Data. Ser. Natl. Bur. Std. (U.S.) Vol. 1 (1966).

14. G. Herzberg, Molecular Spectra and Molecular Structure Vol. III, 2d ed. (Van Nostrand), 1950, p. 283.

15. C. R. Brundle and D. W. Turner, Intl. J. Mass Spectrom. and Ion Phys. 2, 195 (1969).

16. J. F. Mulligan, J. Chem. Phys. 19 347(1951).

17. S. D. Peyerimhoff, R. J. Buenker, and J. L. Whitten, J. Chem. Phys. 46, 1707(1967).

18. R. S. Mulliken, J. Chem. Phys. 3, 720 (1935).

19. E. J. Stone and E. C. Zipf,

TABLE I. ELECTRON GUN PARAMETERS*

Electrode	Potential	Aperture diameter (mm)
Filament F	$-V_o$	
Grid G	$-0.6\,V_o$	$d_1 = 1.5$
Anode A	$+4.3\,V_o$	$d_2 = 1.5$
		$d_3 = 6.3$
Electrode L	$+4.3\,V_o$	
Decelerator P	0	$d_4 = 6.3$
Collision Chamber	0	$d_5 = 3.2$
Electron Collector	+ 15 volt	

*See also Fig. 1 and text.

TABLE II. ABSOLUTE EMISSION CROSS SECTIONS FOR MULTIPLETS OF OI, CI, AND CII PRODUCED BY ELECTRON IMPACT (100 eV) ON CO_2.

	This work	Ajello	Sroka
OI 1304 Å	*1.04(-18) ± 18%	* 7.56(-19)±30%	*5.7(-19)
CI 1329 Å	*2.67(-19) ± 21%	2.50(-19)	--
CI 1561 Å	*7.50(-19) ± 30%	6.79(-19)	--
CI 1657 Å	*1.45(-18) ± 23%	1.31(-18)	--
CII 1324 Å	1.33(-20) ± 23%	---	---
CII 1335	*7.60(-19) ± 22%	* 7.6(-19)	*8.8(-19)

* = excitation function presented.

TABLE III. COMPARISON OF RESULTS FOR THE OI 1304 Å MULTIPLET

	This Work	Ajello[a]	Sroka[b]
Threshold	21 ± 2	21 ± 2	21.5
2nd Threshold	~45	35	~45
peak	~110	100	160-175

a. Ref. 7.

b. Ref. 8.

TABLE IV

Appearance Potentials for Atomic VUV Emission Features Produced by Dissociative Excitation of CO_2.

Multiplet	Possible configuration of Dissociation Fragments	Minimum Appearance Potential, eV	
		Theoretical	Observed
OI 1304Å	$OI(3s\ ^3S) + CO(A^1\pi)$	23.00	
	$OI(3s\ ^3S) + CO(a^3\pi)$	20.98	21
	$OI(3p\ ^3P) + CO(X^1\Sigma^+)$	16.43 (a)	
	$OI(3s\ ^3S) + CO(X^1\Sigma^+)$	14.97 (b)	
CI 1329Å	$CI(2s2p^3\ ^3P^o) + 2OI(2p^4\ ^3P)$	25.90	24
	$CI(2s2p^3\ ^3P^o) + O_2(X^3\Sigma_g^-)$	20.82	
CI 1561Å	$CI(2s2p^3\ ^3D^o) + 2OI(2p^4\ ^3P)$	24.51	~26
	$CI(2s2p^3\ ^3D^o) + O_2(X^3\Sigma_g^-)$	19.43	
CI 1657	$CI(3s\ ^3P^o) + 2\ OI(2p^4\ ^3P)$	24.05	~25
	$CI(3s\ ^3P^o) + O_2(^3\Sigma_g^-)$	18.97	
CII 1335Å	$CII(2s2p^2\ ^2D) + 2\ OI(2p^4\ ^3P)$	37.11	~44
	$CII(2s2p^2\ ^2D) + OI(2p^4\ ^1D) + OI(2p^4\ ^3P)$	39.07	
	$CII(2s2p^2\ ^2D) + 2OI(2p^4\ ^1D)$	41.03	
	$CII(2s2p^2\ ^2D) + OI(2p^4\ ^1S) + OI(2p^4\ ^3P)$	41.30	
	$CII(2s2p^2\ ^2D) + OI(2p^4\ ^1S) + OI(2p^4\ ^1D)$	43.26	
	$CII(2s2p^2\ ^2D) + 2OI(2p^4\ ^1S)$	45.47	

a. The $OI(2p\ ^3P)$ cascades to $OI(3s\ ^3S)$ through emission of a photon at 8447Å. In one very good data run we saw a feature which had a threshold at ~16 eV and a cross section of $\sim 1 \times 10^{-20}$ cm^2. The shape seemed to peak near threshold. We have not included this feature in Fig. 2 since we had trouble reproducing the observation.

b. This combination of final states can arise only from a Σ^- intermediate CO_2^* state. We can therefore exclude this set of final states since $\Sigma^+ \rightarrow \Sigma^-$ transistions are forbidden by electric dipole interaction.

TABLE V

A COMPARISON OF SALIENT FEATURES OF THE CII 1335 Å CROSS SECTION.

	This Work	Ajello[a]	Sroka[b]
Threshold	~44 eV	~45 eV	~45 eV
Peak	~175 eV	~170 eV	~170 eV
σ(170 eV)	10.0(-19)cm^2	8.3(-19)cm^2	13.5(-19)cm^2

a. Ref. 7.

b. Ref. 8.

LIST OF FIGURES

Fig. 1. Schematic diagram of the electron gun showing the filament (F), grid (G), anode (A), lens (L), final electrode (P), and the apertures (d_1, d_2, d_3, d_4, d_5).

Fig. 2. Absolute cross section for dissociative excitation of the OI 1304 Å resonance multiplet by electron impact on CO_2. The solid curve represents the smoothed data.

Fig. 3. Absolute cross section for dissociative excitation of the OI 1304 Å resonance multiplet by electron impact on CO_2: --- Ajello, ----- Sroka, ——— present results.

Fig. 4. Partial term level diagram of CI and CII showing the multiplets observed in this work.

Fig. 5. Absolute cross section for dissociative excitation of the CI 1329 Å multiplet by electron impact on CO_2. The solid curve represents the smoothed data.

Fig. 6. Absolute cross section for dissociative excitation of the CI 1561Å multiplet by electron impact on CO_2. The dashed curve represents the contribution of the (1,1) vibrational band of the CO fourth positive group. The solid curve represents the smoothed data.

Fig. 7. Absolute cross section for dissociative excitation of the CI 1657Å multiplet by electron impact on CO_2. The dashed curve represents the contribution of the (0,2) vibrational band of the CO fourth positive group. The solid curve represents the smoothed data.

Fig. 8. Absolute cross section for dissociative excitation of the CII 1335 Å multiplet by electron impact on CO_2. The solid line represents the smoothed data.

Fig. 9. Comparison of cross sections measured for dissociative excitation of the CII 1335 Å multiplet by electron impact on CO_2: ----- Ajello, ——·—— Sroka, ———— present results.

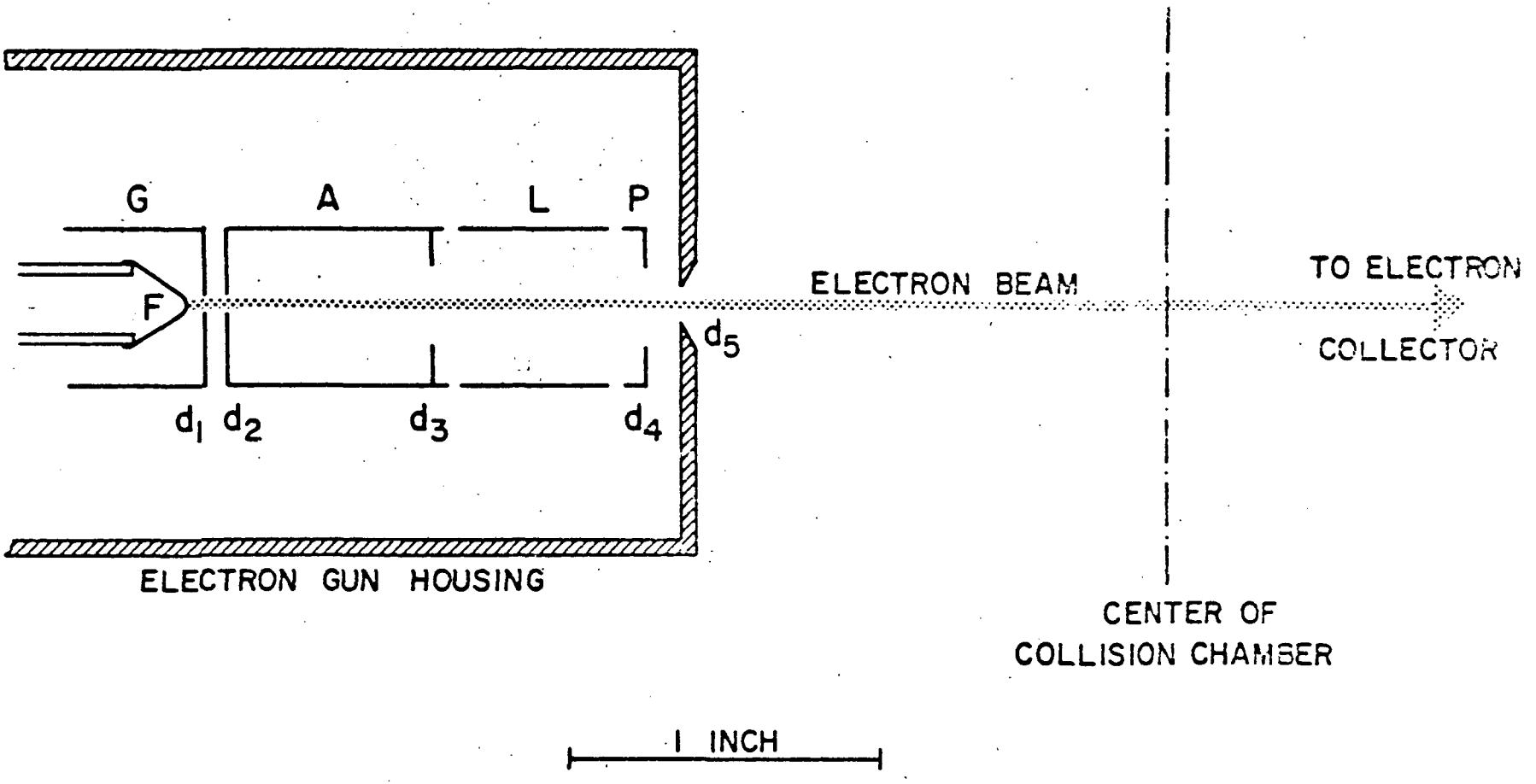

G
A
L
P
F
ELECTRON BEAM
TO ELECTRON
COLLECTOR
d_5
d_1 d_2
d_3
d_4
ELECTRON GUN HOUSING
CENTER OF
COLLISION CHAMBER
1 INCH

Figure 1

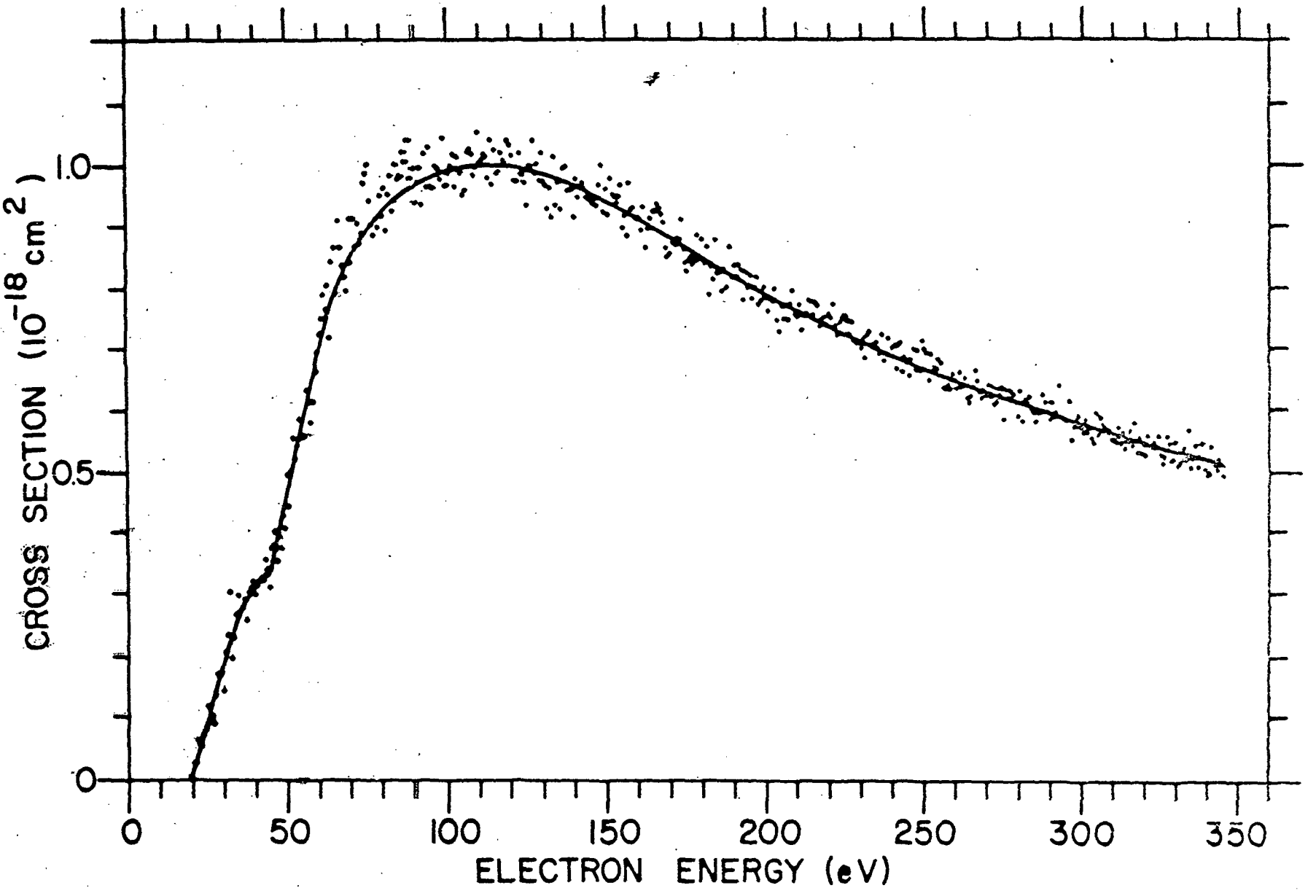

CROSS SECTION (10^{-18} cm^2)
1.0
0.5
0
0
50
100
150
200
250
300
350
ELECTRON ENERGY (eV)

Figure. 2

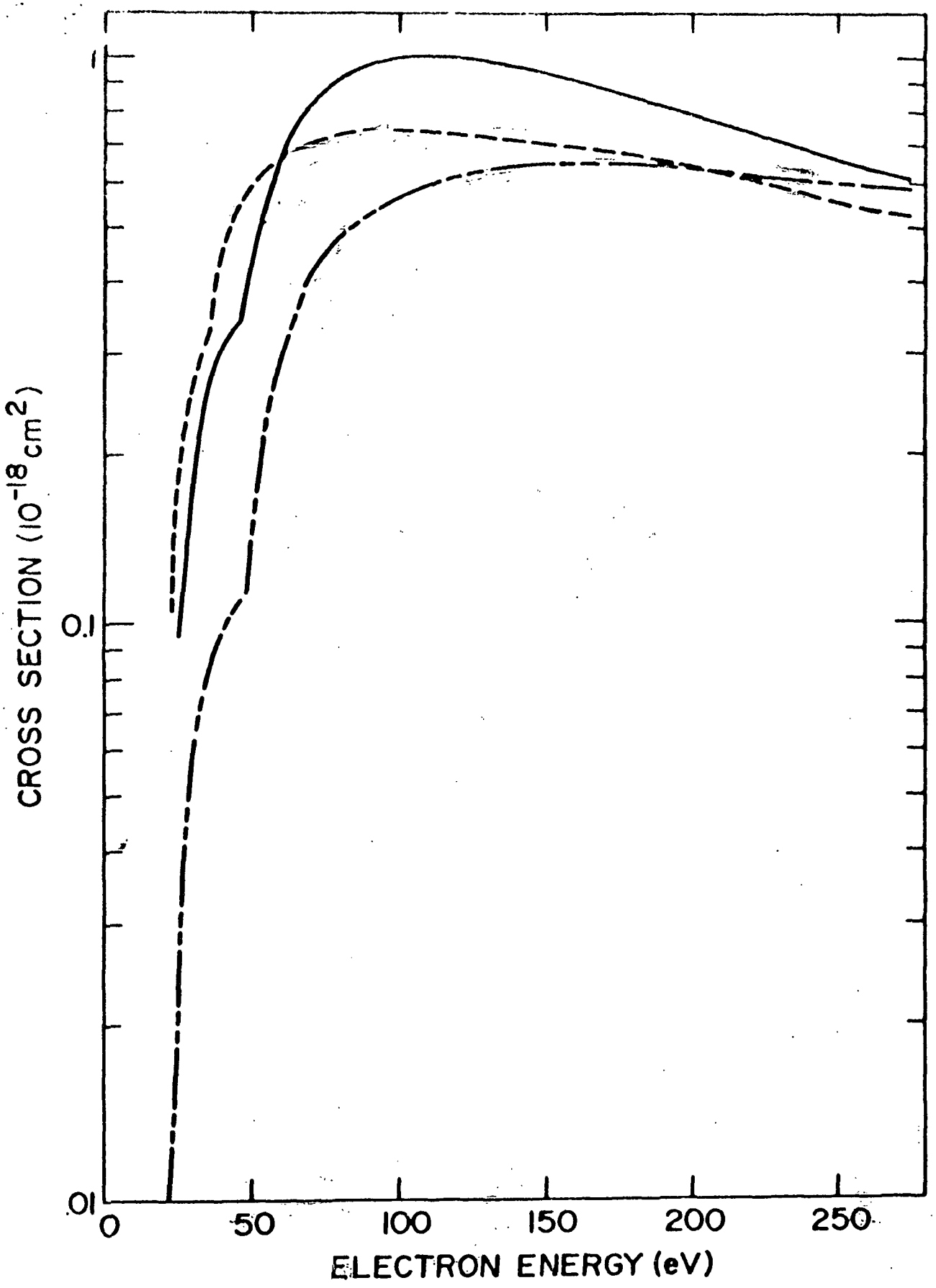

CROSS SECTION (10^{-18} cm^2)
1
0.1
.01
0
50
100
150
200
250
ELECTRON ENERGY (eV)

Figure 3

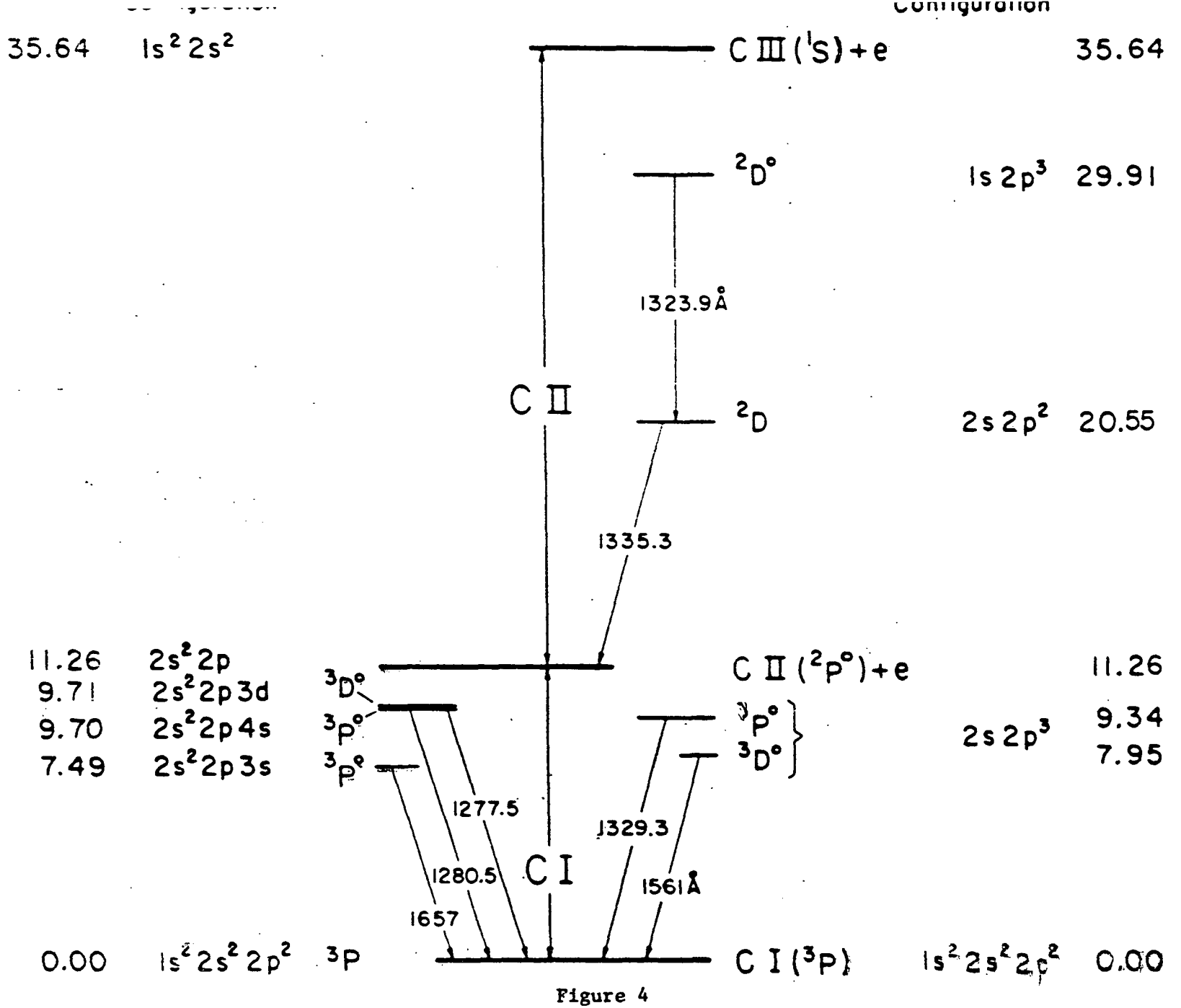

Configuration
35.64 1s² 2s²
C III (¹S) + e
35.64
²D°
1s 2p³ 29.91
1323.9Å
C II
²D
2s 2p² 20.55
1335.3
11.26 2s² 2p
C II (²P°) + e
11.26
9.71 2s² 2p 3d
³D°
9.70 2s² 2p 4s
³P°
7.49 2s² 2p 3s
³P°
³P°
³D°
2s 2p³
9.34
7.95
1277.5
1329.3
1280.5
C I
1561Å
1657
0.00 1s² 2s² 2p² ³P
C I (³P)
1s² 2s² 2p²
0.00

Figure 4

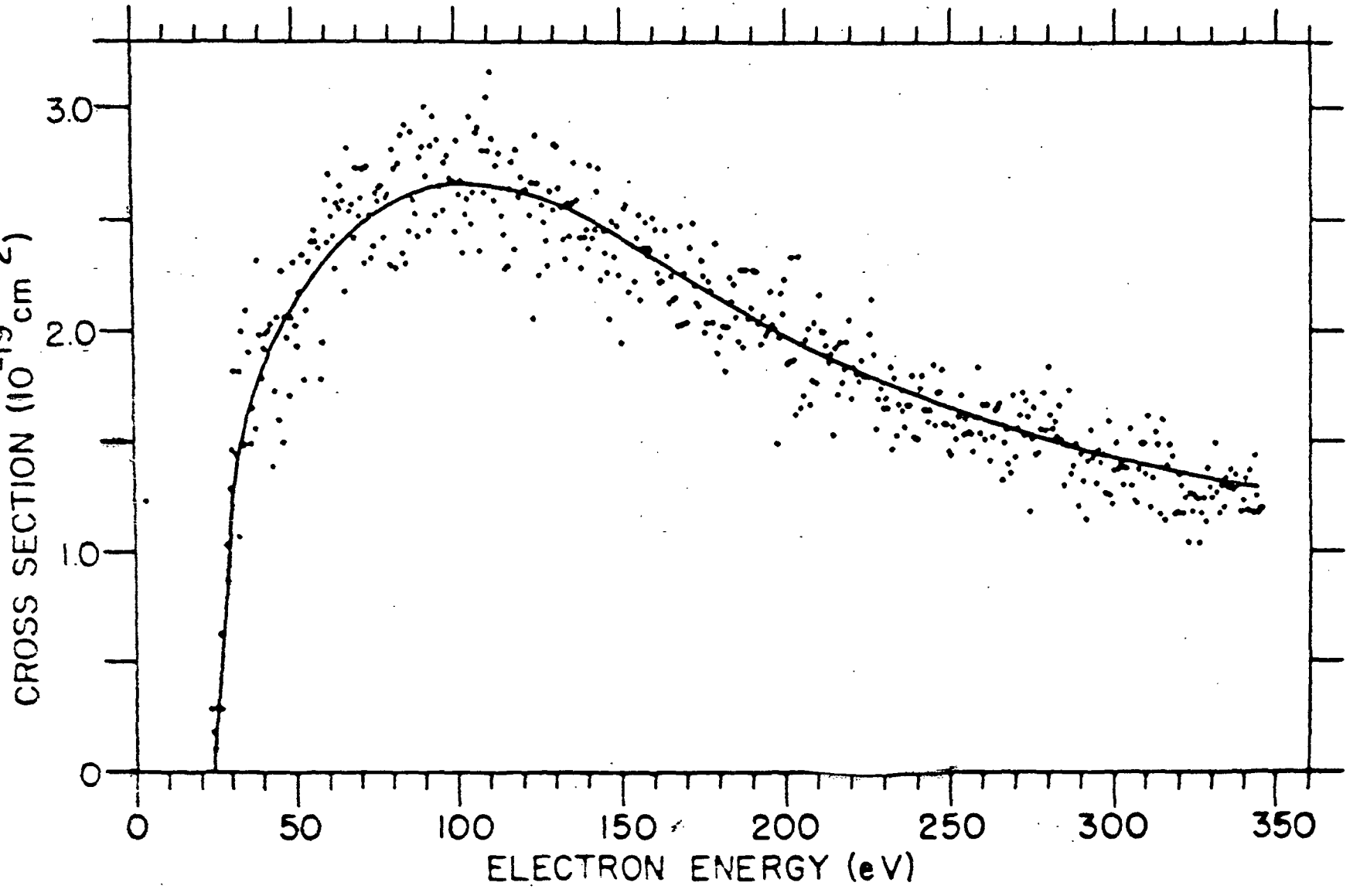

CROSS SECTION (10^{-19} cm^2)
3.0
2.0
1.0
0
0
50
100
150
200
250
300
350
ELECTRON ENERGY (eV)

Figure 5

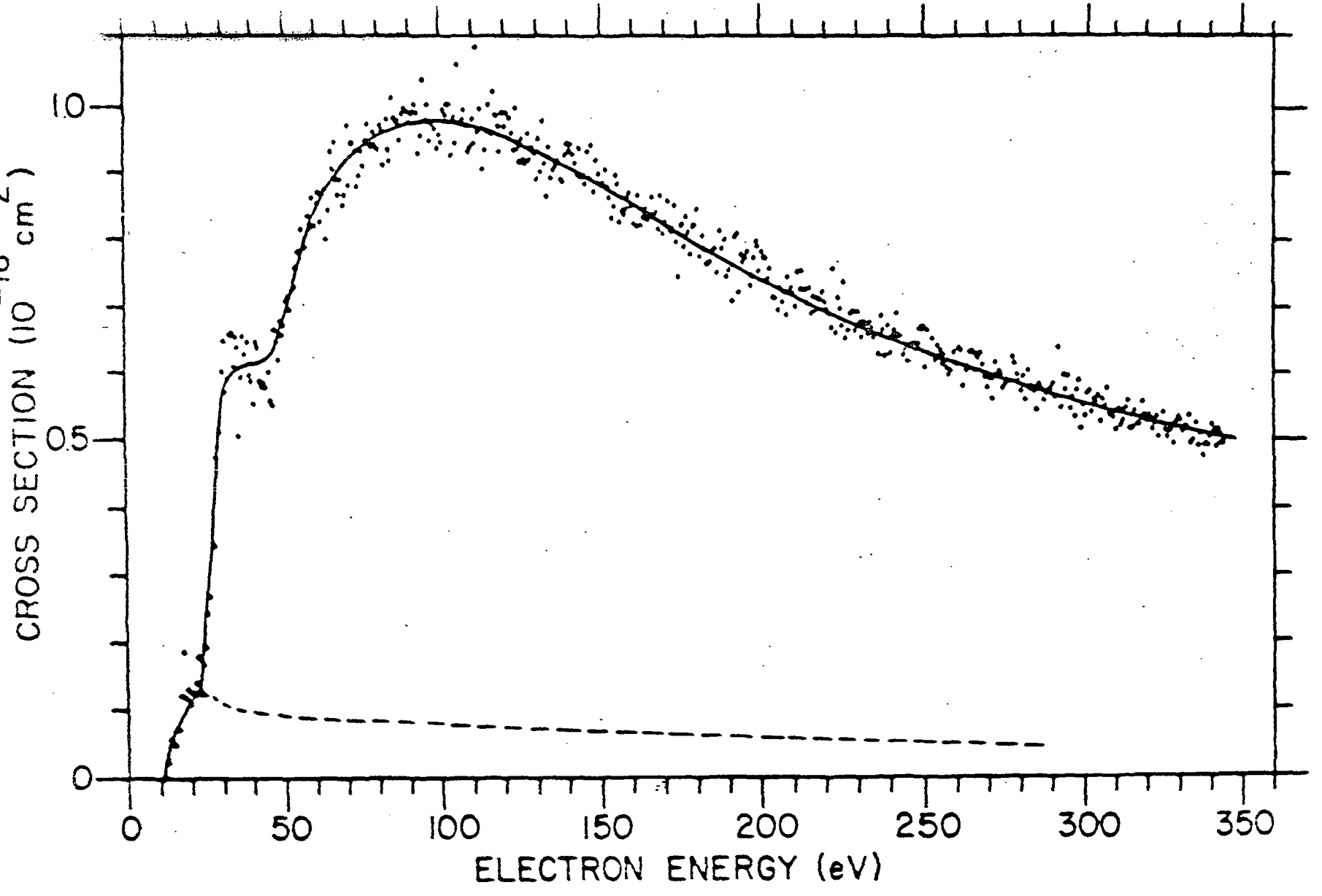

CROSS SECTION (10^{-18} cm^2)
1.0
0.5
0
0
50
100
150
200
250
300
350
ELECTRON ENERGY (eV)

Figure 6

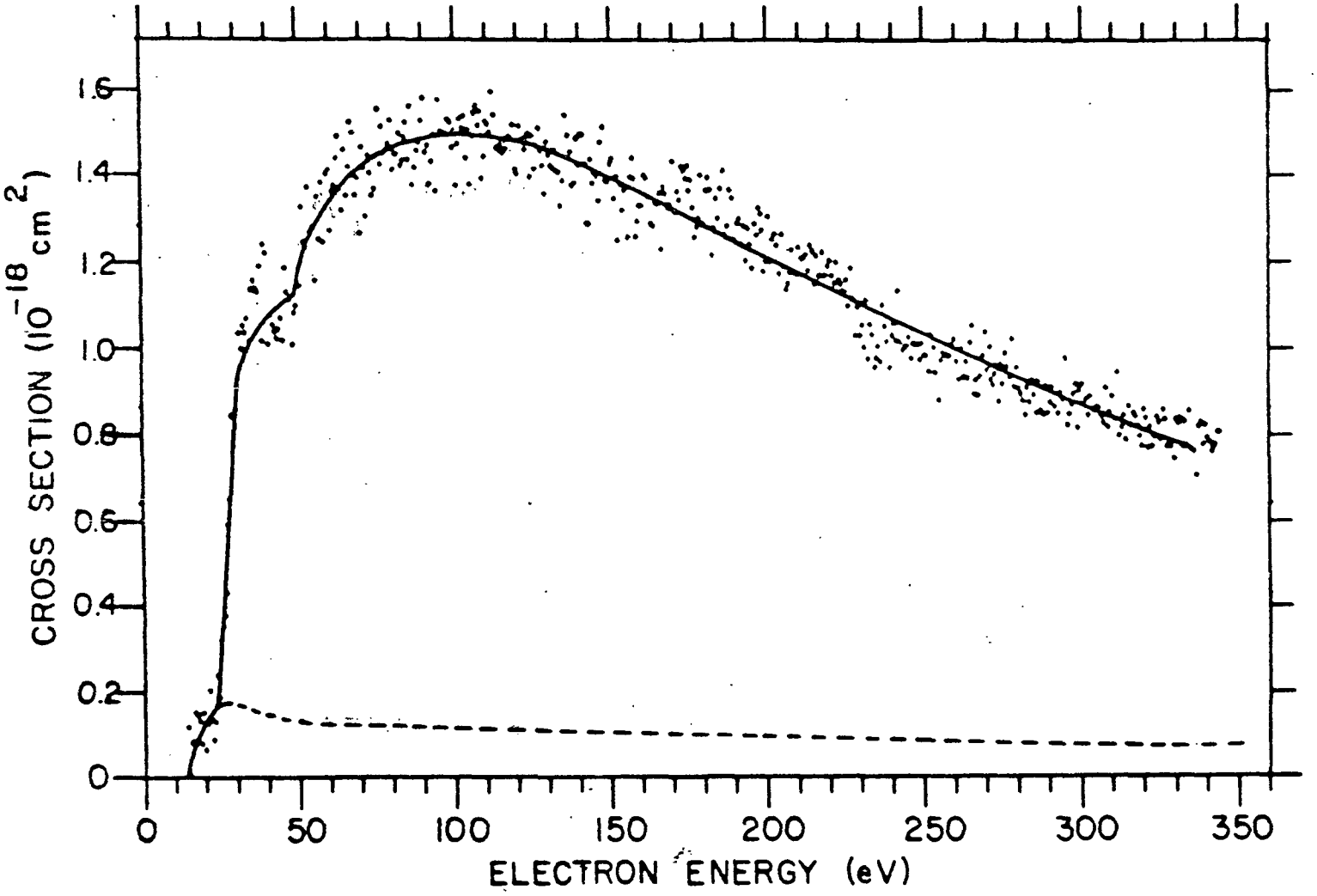

CROSS SECTION (10^{-18} cm^2)
1.6
1.4
1.2
1.0
0.8
0.6
0.4
0.2
0
0
50
100
150
200
250
300
350
ELECTRON ENERGY (eV)

Figure 7

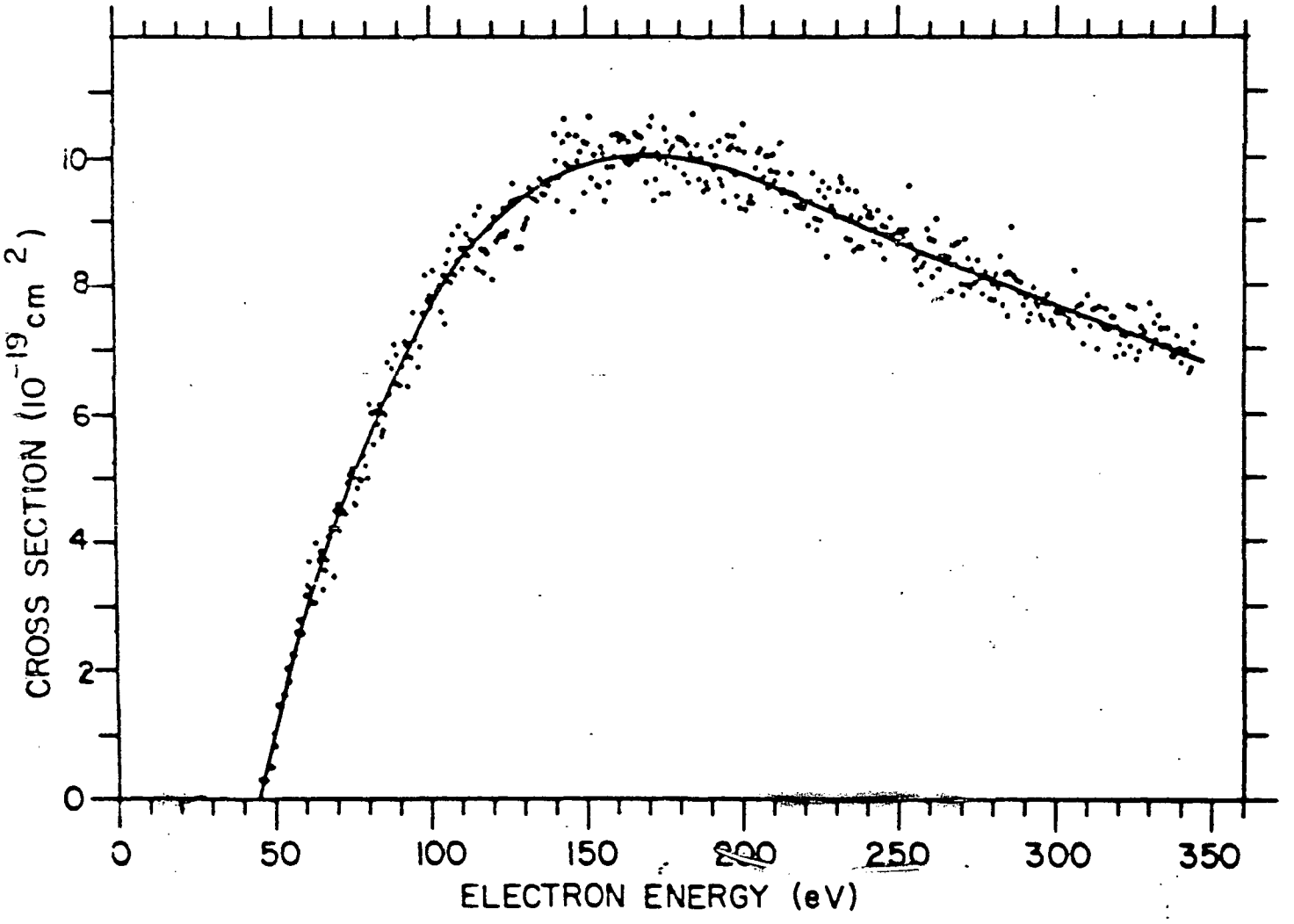

CROSS SECTION (10^{-19} cm^2)
0
2
4
6
8
10
0
50
100
150
200
250
300
350
ELECTRON ENERGY (eV)

Figure 8

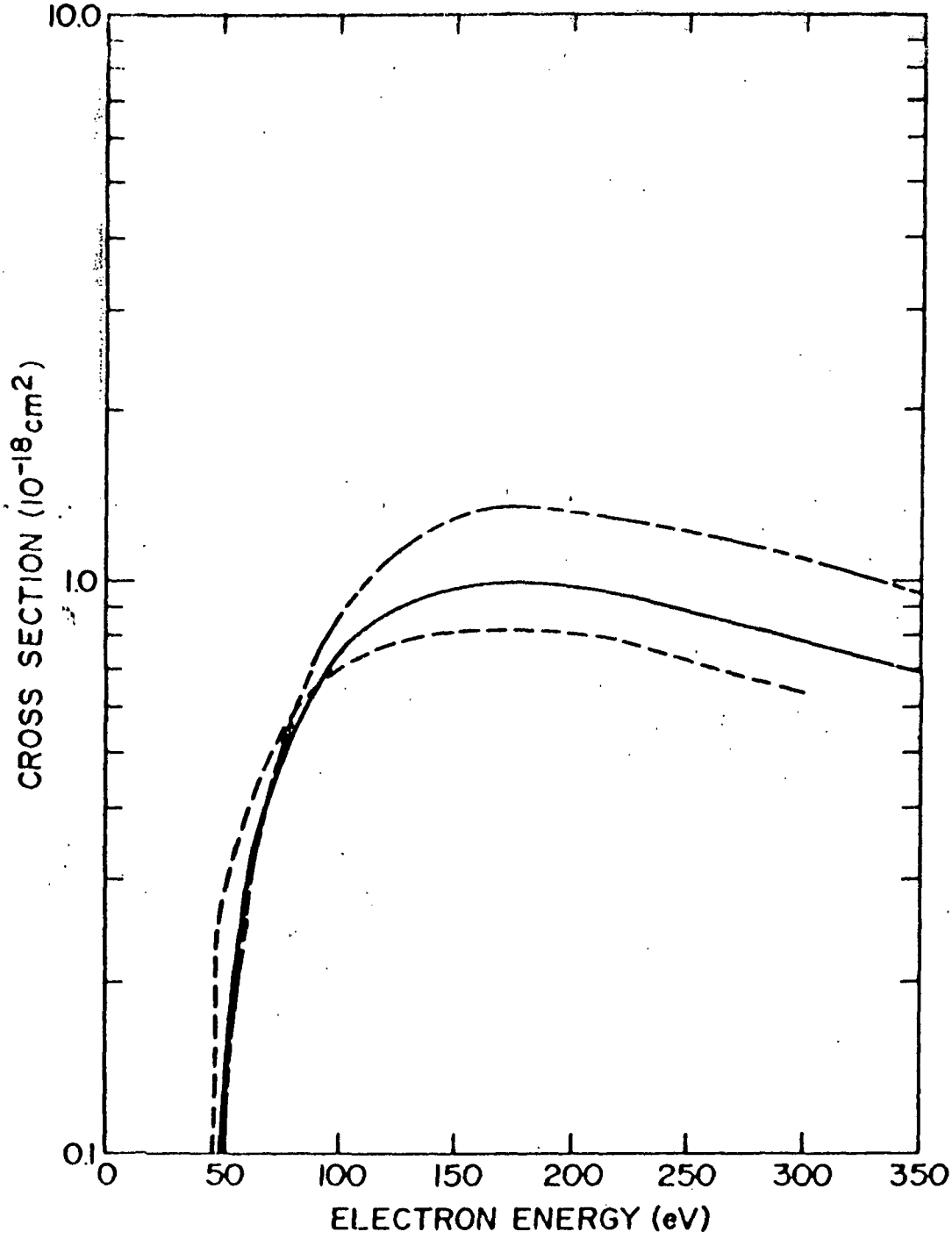

10.0
1.0
0.1
CROSS SECTION (10^{-18}cm^2)
0
50
100
150
200
250
300
350
ELECTRON ENERGY (eV)

Figure 9